Zeitschrift: Eclogae Geologicae Helvetiae
Herausgeber: Schweizerische Geologische Gesellschaft
Band: 97 (2004)
Heft: 2

Artikel: Deformation at the Leventina-Simona nappe boundary, Central Alps, Switzerland
Autor: Timar-Geng, Zoltan / Grujic, Djordje / Rahn, Meinert
DOI: https://doi.org/10.5169/seals-169112

0012-9402/04/020265-14
DOI 10.1007/s00015-004-1121-4
Birkhäuser Verlag, Basel, 2004

Eclogae geol. Helv. 97 (2004) 265–278

Deformation at the Leventina-Simano nappe boundary, Central Alps, Switzerland

ZOLTAN TIMAR-GENG[1,*], DJORDJE GRUJIC[2] & MEINERT RAHN[3,**]

Key words: Lepontine Alps, Leventina nappe, Simano nappe, quartz texture, apatite fission track dating, deformation history

ABSTRACT

In the Leventina valley of southern Switzerland a mylonite zone marks the boundary between Leventina and Simano nappe. Quartz textures and deformation microstructures are used to obtain information about the deformation conditions and kinematics in the mylonite zone. The *c*-axis patterns give evidence for a non-coaxial finite strain with a high scatter of the constructed shear directions. During texture formation the temperature conditions were in the range of 400–630 °C. Structural elements observed in the Leventina-Simano nappe boundary area are integrated into the well-established regional deformation history of the Lepontine dome. On the basis of the kinematics and metamorphic conditions, the last non-brittle increment of the progressive deformation that caused the crystallographic preferred orientation in the quartz tectonites is assigned to the late second to third regional deformation phase. Under brittle to brittle-plastic conditions the mylonite zone was reactivated with a top-to-the-WNW shearing direction. This reactivation is possibly kinematically connected to other major orogen-parallel oriented extensional structures formed in the Miocene, like the Simplon and the Brenner shear zone and fault.

Apatite fission track ages (~3.7–10 Ma) across the nappe boundary are similar to the regional data range, but show a negative age-altitude trend. The fission track data combined with structural and kinematic data indicate that there was no considerable amount of vertical displacement along the Leventina-Simano nappe boundary during or after Mid-Miocene. For the negative age-elevation relationship, interplay between exhumation and landscape evolution is suggested.

ZUSAMMENFASSUNG

Eine Mylonitzone stellt in der Leventina (Tessin) die Grenze zwischen der Leventina- und der Simano-Decke dar. Quarztexturen und Deformations-Mikrostrukturen wurden untersucht, um Information über die Deformationsbedingungen und Kinematik in der Mylonitzone zu gewinnen. Die *c*-Achsengefüge zeigen eine nicht-koaxiale finite Verformung mit einer markanten Streuung der konstruierten Scherrichtungen. Während der Texturbildung herrschten Temperaturbedingungen von 400–630 °C. Die beobachteten Strukturelemente im Gebiet der Deckengrenze werden in die bekannte regionale Deformationsgeschichte des lepontinischen Domes eingeordnet. Aufgrund der Kinematik und den metamorphen Bedingungen wird das letzte nicht-spröde Inkrement der progressiven Deformation, das die kristallographisch bevorzugte Orientierung in den Quarztektoniten hervorrief, der späten zweiten bis dritten regionalen Deformationsphase zugeordnet. Die Mylonitzone wurde danach unter spröden bis spröd-plastischen Bedingungen und einem WNW-gerichteten Schersinn reaktiviert. Diese Reaktivierung ist möglicherweise kinematisch mit anderen grossen orogenparallel orientierten miozänen Extensionsstrukturen wie der Simplon- und der Brenner-Linie, verknüpft.

Spaltspurenalter an Apatit (~3,7–10 Ma) von quer zur Deckengrenze gesammelten Proben stimmen mit dem regionalen Datensatz überein, zeigen aber eine negative Alters-Höhen-Korrelation. Die Spaltspurendaten deuten zusammen mit den strukturgeologischen und kinematischen Daten darauf hin, dass es keinen bedeutenden Vertikalversatz entlang der Leventina-Simano-Deckengrenze während oder nach dem mittleren Miozän gab. Für die negative Alters-Höhen-Korrelation wird ein Zusammenspiel zwischen Exhumierung und topographischer Entwicklung vorgeschlagen.

1. Introduction

The late-stage tectonic and exhumation history of the Central Alps has been the subject of many recent studies (e.g. Hurford et al. 1989; Grasemann & Mancktelow 1993; Schlunegger & Willett 1999; von Eynatten et al. 1999; Kuhlemann et al. 2001; Bernet et al. 2001). Tectonic denudation along low-angle normal faults is thought to represent the most prominent process that enabled the Miocene exhumation of some Penninic basement complexes in the Alps (Kuhlemann et al. 2001). Within

[1] Geologisches Institut, Albert-Ludwigs-Universität Freiburg, Albertstr. 23b, D–79104 Freiburg, Germany.
[2] Department of Earth Sciences, Dalhousie University, Halifax, NS B3H 3J5, Canada.
[3] Institut für Mineralogie, Petrologie und Geochemie, Albert-Ludwigs-Universität Freiburg, Albertstr. 23b, D-79104 Freiburg, Germany.
* Present address: Geologisch-Paläontologisches Institut, Bernoullistr. 32, CH–4056 Basel, Switzerland.
** Present address: HSK, CH–5232 Villigen-HSK, Switzerland.

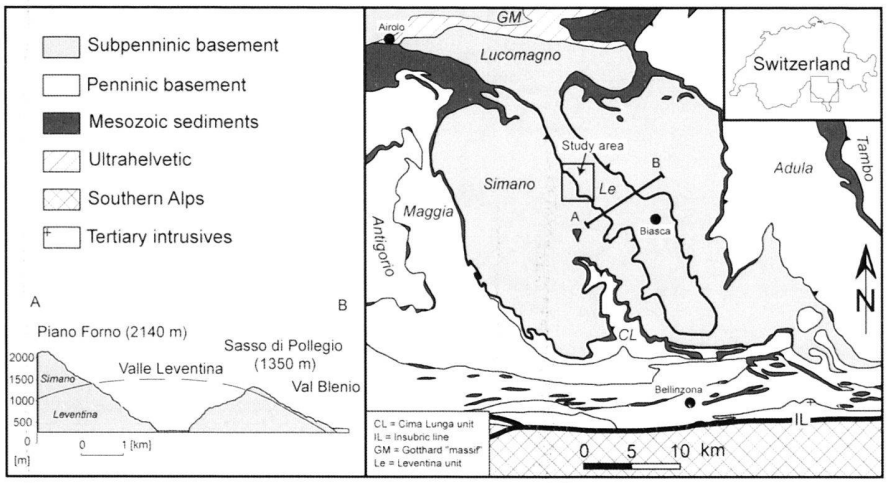

Fig. 1. Tectonic map of the eastern Lepontine Alps after Spicher (1980). On the left: schematic cross-section across the Ticino culmination after Casasopra (1939) and our data.

the Central and Eastern Alps two major normal faults were found to be closely linked to the exhumation of deeply seated basement units: the Simplon fault zone (e.g. Steck 1980, 1984, 1987, 1990; Mancktelow 1985, 1990, 1992; Mancel & Merle 1987; Steck & Hunziker 1994) and the Brenner fault zone (e.g. Behrmann 1988; Selverstone 1988, 1993; Axen et al. 1995; Selverstone et al. 1995; Fügenschuh et al. 1997). Both shear- and fault zones are located on the western side of their exhumed domes (Lepontine Dome and Tauern Window respectively) and accommodate an orogen-parallel extension. The diverging displacement between Monte Rosa and Adula units since ca. 35 Ma, caused probably by divergent displacement vectors between the western and central Alps, can be responsible for the orogen-parallel stretching and exhumation of the Lepontine Dome by inducing normal faulting across the Simplon fault zone (Schmid & Kissling 2000). The lack of prominent extension structures on their eastern side suggests that the exhumation of these domes may have been asymmetric. In search for contemporaneous top to the east extensional elements, the Forcola fault (Meyre et al. 1998) and the Turba mylonite zone (Nievergelt et al. 1996) were proposed to play a similar or subordinate role during exhumation of the basement domes (Schlunegger & Willett 1999).

Alternatively, nappe boundaries within the Lepontine dome could have been reactivated as low-angle normal faults to accommodate the differential uplift and exhumation in the central Alps. This study considers the question, whether the mylonite zone between Leventina nappe (footwall) and Simano nappe (hanging wall) may have been active during post-metamorphic doming and exhumation of the Lepontine Alps.

The structural and kinematic characteristics of the shear zone separating the two nappes are described and apatite fission-track data across the shear zone are presented. These data are combined to demonstrate that the shear zone is a pre-Neogene structure reactivated in the Neogene as a brittle to plastic shear zone with negligible vertical displacement.

2. Geological setting and deformation history

The Leventina and Simano nappes are located in the eastern part of the Lepontine dome in the Central Alps and represent the lowermost tectonic units exposed by erosion along the Ticino valley (Casasopra 1939) (Fig. 1). These nappes correspond to the southernmost pre-Alpine basement of the European margin (e.g. Froitzheim et al. 1996) and are termed, together with the Gotthard massif, as the Subpenninic complex (Milnes 1974) or Infrapenninic (Trümpy 1980). Together with the other Penninic units these nappes have been detached and transported towards the northern foreland during the Eocene. A 200–250 m thick mylonite zone separates the Leventina nappe (bottom) and the Simano nappe (top) (Fig. 2). The protoliths of the mylonite zone are Leventina gneisses and metasediments of the Late Palaeozoic to Mesozoic sedimentary cover. The base of the Simano nappe is not significantly sheared. However, a mylonitised zone is located at the top of the nappe, at the boundary to the Adula nappe (Rütti 2001).

The Leventina nappe consists mainly of granitic orthogneisses with a more or less preserved magmatic fabric at its base, and an augen-gneiss-texture close to the shear zone. The Simano nappe is made up of metapelites with the mineral assemblage Qtz + Kfs + Bt + Ms + Pl ± Grt ± St ± Ky (abbreviations after Kretz 1983) and subordinate amphibolites. Mesozoic metasediments are the typical nappe separators in the Central Alps (e.g. Niggli et al. 1936). These Triassic quartzites and marbles are only rarely found in the study area because southward, towards the cores of the nappe-separating synclines, the sediments are progressively boudinaged into discontinuous lenses (see e.g. Spicher 1980).

Early in the post-collisional tectonic stage the whole Lepontine dome experienced amphibolite grade metamorphism during the Oligocene (e.g. Jäger 1973; Steck & Hunziker 1994; Frey & Ferreiro Mählmann 1999). At the Leventina-Simano boundary in the study area this Lepontine metamorphism reached peak conditions of 600 – 650 °C and 6.0 – 6.5 kbar

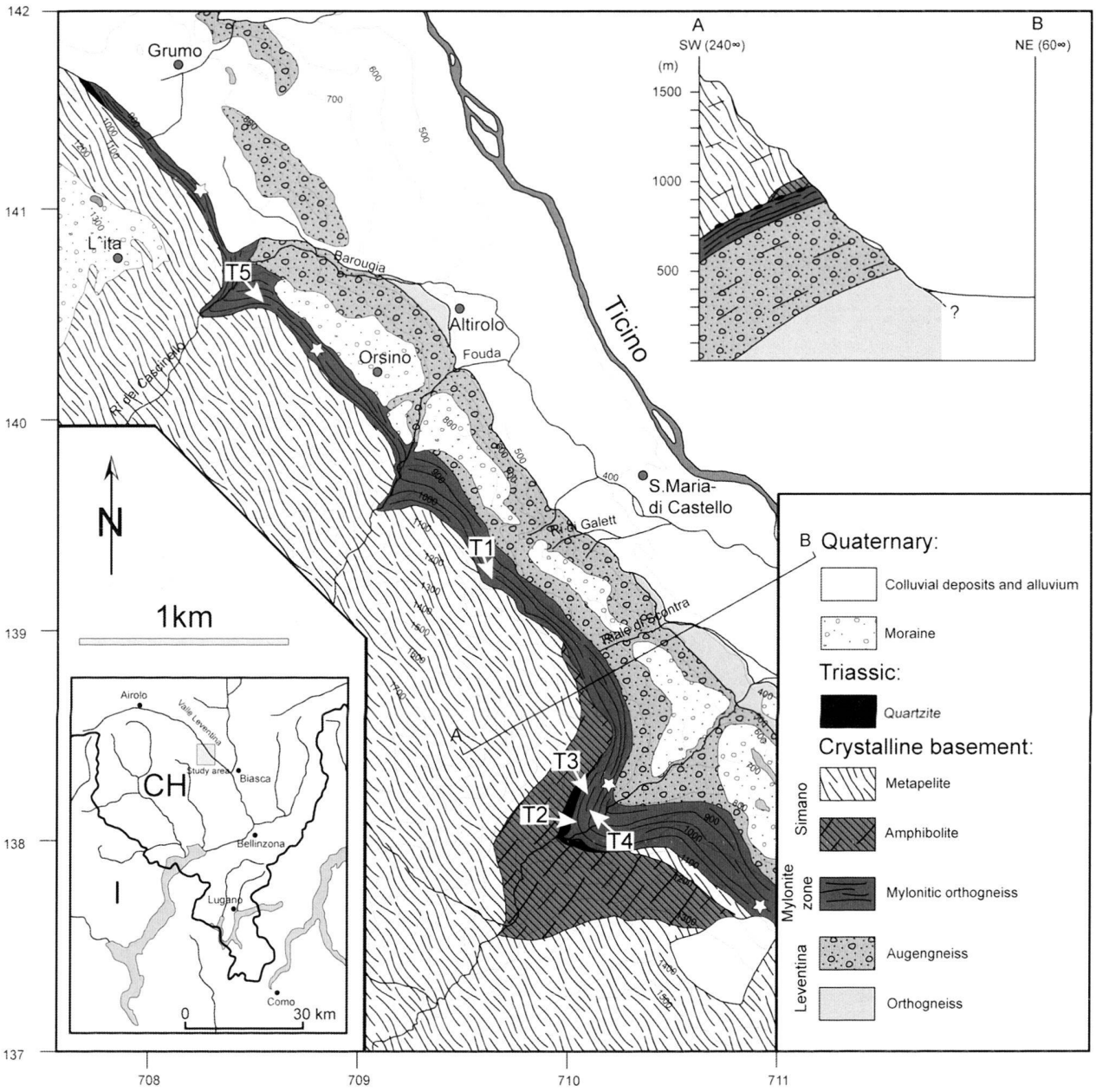

Fig. 2. Geological map of the study area. T1 to T5: Locations of samples collected for U-stage measurements. Small stars in the mylonitic orthogneiss represent pseudotachylite localities (Irouschek & Huber 1982, and this study).

(Todd & Engi 1997, their fig. 7). Average P-T conditions at the Simano-Adula nappe boundary during the main thermal event were about 7 kbar and 625 °C (Rütti 2001). Similar results were obtained in the frontal part of the Simano nappe, where metamorphic conditions reached 580–650 °C and >5.5 kbar (Rütti et al. 2001).

The penetrative and polyphase deformation in the Penninic units has been extensively studied (e.g. Preiswerk 1921; Milnes 1974; Grujic & Mancktelow 1996 and references therein; Steck 1998). As a first order approximation, two main plastic deformation events can be recognised in the Lepontine dome. Merle et al. (1989) identified them as a high-temperature deformation (HTD) under amphibolite facies conditions followed by a retrograde deformation (RD) coeval with cooling of the area. Similarly, although with different regional interpretation, Steck (1980, 1984, 1987, 1990) distinguished two perpendicular directions of synmetamorphic extension, the earlier related to the NW-directed thrusting, the later corre-

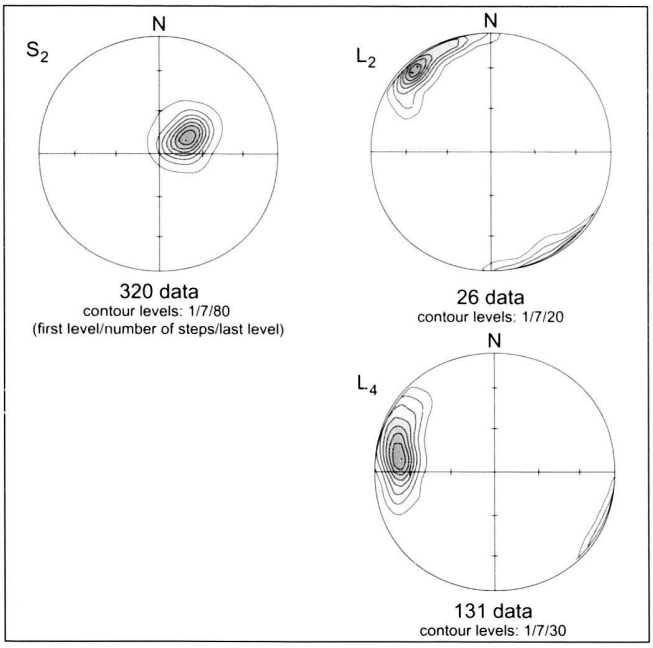

Fig. 3. Contoured pole-density diagrams (equal area, lower hemisphere projection): D_2 foliation (S_2), D_2 mineral and stretching lineation (L_2), and D_4 brittle lineation/ slickenlines (L_4).

sponding to the S to SW-directed extension. Based on compilation of published and unpublished data, and on regional correlation of folding events and metamorphism, Grujic & Mancktelow (1996) established a sequence of five Alpine folding phases. However, ambiguities in the interpretation of some first order structures allow for some alternative deformation histories for the Lepontine area (e.g. Steck 1998). In this study, structural elements observed in the Leventina-Simano nappe boundary area (Fig. 3) were arranged according to the scheme provided by Grujic & Mancktelow (1996). This scheme, together with the schemes provided by Merle et al. (1989) and Steck (1984, 1990), offers a correlation between deformation phases and the associated metamorphic conditions in the different areas of the Lepontine area. Our field observations suggest that the mylonite zone along the Leventina-Simano nappe boundary represents an area with a long deformation history.

3. Deformation of quartz tectonites

Microtectonic studies of quartz provide information about the last plastic increment of progressive deformation in a volume of rock (Law 1990; Schmid 1994; Passchier & Trouw 1998). Microstructures document recovery processes and dynamic recrystallisation mechanisms whereas the crystallographic preferred orientation (in the following quartz textures) offers information about the deformation conditions, finite strain and kinematics within a ductile shear zone. In this study, quartz deformation microstructures and *c*-axis textures are used for a

Tab. 1. Tectonites collected for U-stage measurements. Coordinates are from the Swiss national topographic map 1:25 000, # 1273 Biasca.

Sample	Lithology	Geographic position
T1	Quartz-mylonite, 80% quartz	709670/139290 altitude: 860 m
T2	Quartz-mylonite, 80% quartz	709950/138120 altitude: 940 m
T3	Quartz-mylonite, 80% quartz	710050/138240 altitude: 890 m
T4	Quartz-mylonite, 80% quartz	710070/138250 altitude: 870 m
T5	muscovite-K-feldspar-plagioclase-quartz-proto-mylonite, <<80 % quartz	708540/140560 altitude: 910 m

structural interpretation of the Leventina-Simano mylonite zone.

3.1 Quartz textures

Five samples were collected in the shear zone between the Leventina and the Simano nappe (Tab. 1 and Fig. 2) to study the tectonic history of this high strain nappe contact. The samples are quartz tectonites with well-developed mylonitic foliation and stretching lineation. In four samples the quartz content is at least 80%, the fifth sample is a muscovite-K-feldspar-plagioclase-quartz-mylonite. The samples were cut perpendicular to the foliation and parallel to the macroscopic stretching lineation (L_2, Fig. 3) to obtain thin sections oriented parallel to the *XZ* plane of the finite strain. These linear and planar texture elements are assumed to be produced during deformation at temperature peak metamorphic conditions, i.e. they are named as S_2 and L_2 by most of the geologists working in the area (e.g. see review by Grujic & Mancktelow (1996) and references therein). Measurements of the quartz *c*-axes were carried out with the help of a universal stage under the polarization microscope. The obtained quartz texture patterns (Fig. 4) are distinctly oblique to the stretching lineation, which is a finite strain feature. The textures were rotated around the *Z* axis into a symmetric position within the equal area projection net, resulting in the central segment of the girdle passing through the centre of the projection. The angle of rotation was used to determine the kinematic direction of shearing by adding (within the corresponding foliation plane) that angle to the attitude of the macroscopic stretching lineation. The rotated quartz textures are presented in Fig. 5.

The quartz *c*-axes (Fig. 5, on the left) and the derived skeleton figures (Fig. 5, on the right) show a stronger (T1, T3, T4) or weaker (T5) lattice preferred orientation. It is difficult to compare T2 to the other samples, because it is coarse-grained mylonite and twice as many measurements were needed as for the other samples. Nevertheless, T2 exhibits a weak lattice preferred orientation, too. The strength of the lattice preferred orientation is suggested by the density distribution of the *c*-axes.

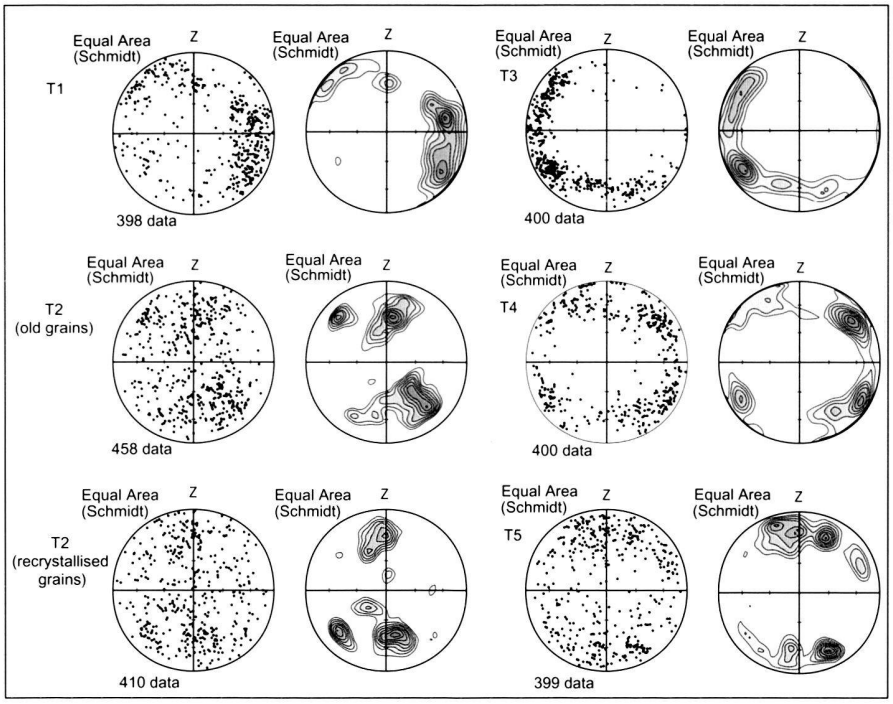

Fig. 4. Quartz *c*-axes distributions (scatter plots and contoured diagrams) of samples T1-T5 (equal area, lower hemisphere projection). Contours in multiples of uniform distribution (see Fig. 5).

3.2 Deformation conditions in the shear zone

Strain

The *c*-axis patterns give evidence for a non-coaxial strain. The *c*-axes girdles in the samples T1, T3 and T4 are asymmetrically oriented with respect to the foliation, i.e. the inferred slip plane (see Passchier & Trouw 1998). Asymmetry is particularly well recognizable in the skeleton figures (Fig. 5). Despite missing central segments of the *c*-axes girdles, an asymmetry is also recognizable in the samples T2 and T5. In all the analysed samples the local maxima of the *c*-axis patterns are likewise asymmetrically distributed with respect to the slip plane.

Samples T1, T3 and T4 show *c*-axis patterns that can be attributed to a type I crossed girdle or a single girdle (Schmid & Casey 1986). No clear crossed girdles are present in the samples T2 and T5, because the central segments are missing. The *c*-axes are scattered around the *Z*-axis, however, a distribution along a small circle is not recognizable. The topology of the *c*-axes may suggest that the deformation took place within the field of flattening strain. This strain geometry is indicated by the absence of a central segment, which is a transition between type I crossed girdle and distribution of *c*-axes along a small circle centered at the *Z* axis (Schmid & Casey 1986, their Fig. 15). It is thus conceivable that the *c*-axis patterns of the samples T2 and T5 represent the result of a combination of coaxial and a non-coaxial strain component that caused the asymmetry of the *c*-axis distribution, i.e. the vorticity number of the deformation was $0<\omega<1$. However, this interpretation has to be taken with caution because missing sections of fabric skeletons may arise from annealing too (Heilbronner & Tullis 2002). Furthermore sample T5 is a polymineralic proto-mylonite with lowest content of quartz grains, which makes its interpretation difficult.

Sense of shear

Quartz *c*-axis patterns are frequently used as a tool to determine the sense of shear or to support an independent determination by other methods (among many others, Simpson & Schmid 1982; Behrmann & Platt 1982; Mancktelow 1987; Grasemann et al. 1999; Stipp et al. 2002). In the case of non-coaxial strain the asymmetry of the quartz *c*-axis pattern to the inferred slip plane (see Passchier & Trouw 1998) serves as a reliable sense of shear indicator. The asymmetry in the examined samples shows a fairly clear picture, however, in the map view there is a high scatter of the constructed kinematic directions. Because the plunge azimuth of the lineation (L_2) varies between north and south, the shear directions (except T5) vary between top-to-the NW and top-to-the SW (Fig. 5). This high scatter of constructed shear directions suggests that the pure shear, i.e. vertical shortening and accompanied extension in a subhorizontal plane, was dominant in a general shear deformation along this high strain zone. Based on the deformation history provided by Grujic & Mancktelow (1996) it is unlikely that the high scatter in shear direction results from later folding events.

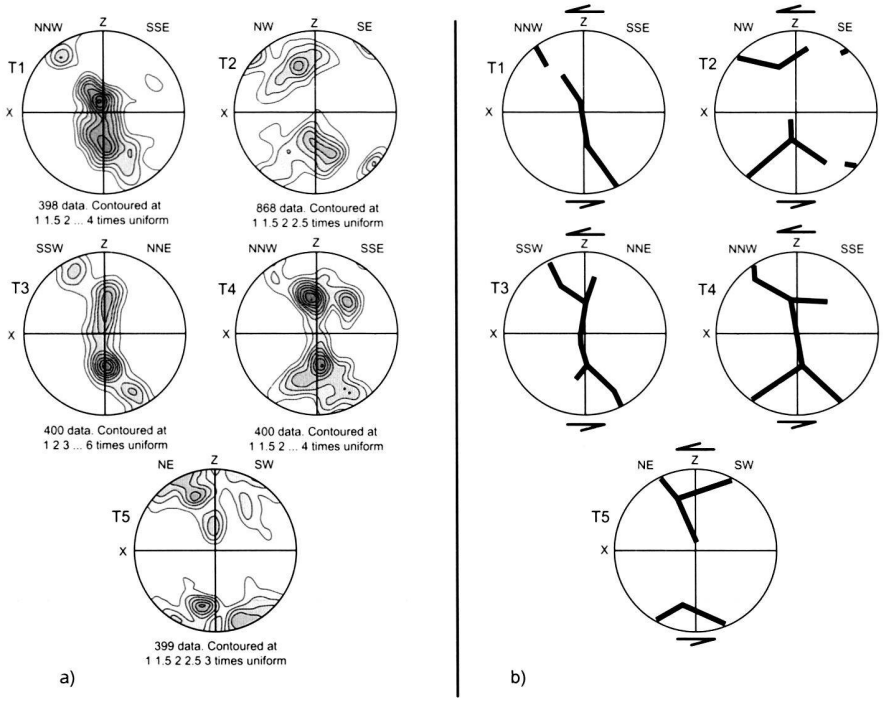

Fig. 5. a) Rotated quartz textures of the investigated samples and b) the inferred fabric skeletons. The rotation axis was the *Z*-axis.

Temperature conditions

From the quartz *c*-axis patterns the active slip systems can be estimated (e.g. Bouchez & Pêcher 1981; Schmid & Casey 1986). The activation of the slip systems is temperature-dependent (Passchier & Trouw 1998; Stipp et al. 2002). Therefore, from the dominance of certain slip systems approximate temperature conditions that prevailed during the texture formation could be inferred. The active slip systems are documented by the formation of discrete maxima and submaxima of the crystallographic axes within particular areas of the diagram (Passchier & Trouw 1998).

Rhomb <a> slip is in all five samples the dominant slip system as suggested by main maxima midway between the centre of the diagram and the periphery. Basal <a> slip is present but less dominant. The activity of this slip system is suggested by submaxima of *c*-axes at the periphery of the diagrams in the samples T1, T2 and T3. Prism <a> slip (indicated by concentration of *c*-axes in the centre of the diagrams) is present in the sample T1, but also decipherable in the samples T3 and T4 (Fig. 5). The change from multiple <a> slip systems to a single active prism <a> slip system occurs at about ~500 °C (Stipp et al. 2002).

From the *c*-axis distributions it can be assumed that the texture formation by combined rhomb and basal ± prism <a> slip has occurred at medium temperature conditions (400 to 500°C) (Passchier & Trouw 1998; Stipp et al. 2002). However, as annealing plays an important role for the maxima-distribution of the pole figures (Heilbronner & Tullis 2002), further information is needed to determine deformation temperature conditions. Deformation microstructures (Fig. 6), too, provide some information about the temperature conditions during deformation (Stipp et al. 2002). Microstructural analysis was performed on samples T1 to T4 on the same thin sections that were subjected to the universal stage measurements. There is evidence both for intracrystalline deformation (patchy undulose extinction) and for dynamic recrystallisation. The observed microstructures (Fig. 6) are characterized by two distinct dynamic recrystallization mechanisms of quartz: subgrain rotation recrystallization (SGR) and grain boundary migration recrystallisation (GBM). Core and mantle structures of porphyroclastic ribbon grains and recrystallized subgrains (Fig 6b) are indicative of SGR. Recrystallized grains are partly arranged in layers oblique to the main foliation (Fig 6b). Highly irregular grain shapes and grain sizes (Fig 6a, c, d) are characteristic for GBM. The combined SGR and GBM mechanisms of quartz indicate medium to high-grade conditions (from ~400 to ~700 °C) (Stipp et al. 2002). The absence of chessboard microstructure (subgrain boundaries parallel to prism and basal planes), which forms above α-β transformation of quartz, constrains the temperature conditions of deformation to the lower temperature GBM sub-zone (from ~500 to ~630 °C) (Stipp et al. 2002). The upper temperature limit is further constrained by the absence of *c*-axis maxima indicative of prism [c] slip.

The combined texture and microstructure indicators therefore suggest that the last increment of ductile deformation at the nappe boundary occurred at greenschist to lower amphibolite facies conditions.

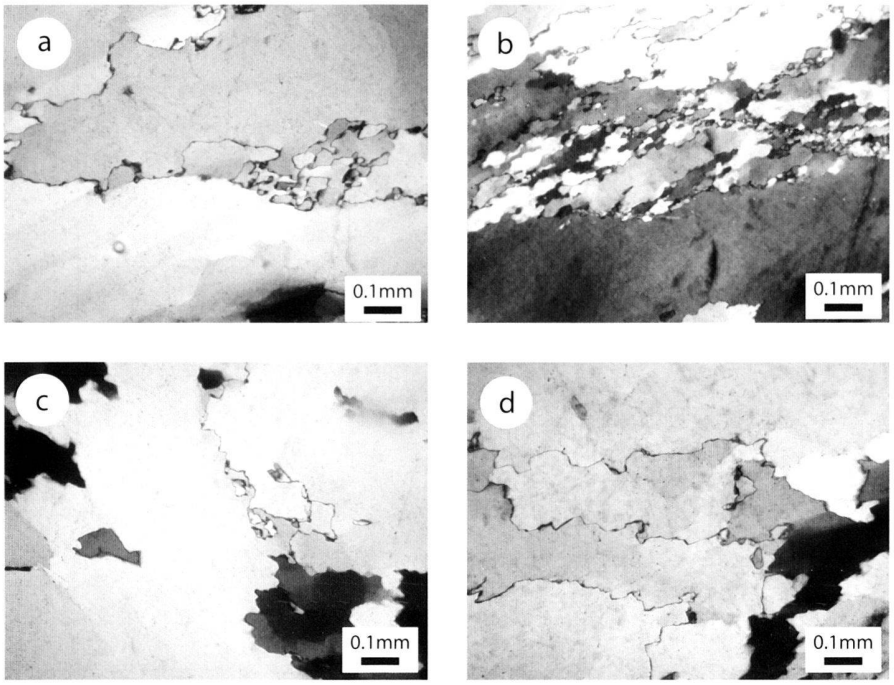

Fig. 6. Characteristic microstructures of samples (a) T3; (b) T2; (c) T1; (d) T4, observed in XZ sections, i.e. perpendicular to foliation and parallel to the stretching lineation. Elongated ribbon grains and recrystallized subgrains (6b) are characteristic for SGR. Interfingering sutures of grain boundaries, irregular grain shapes and grain sizes (6a, c, d) are indicative of GBM.

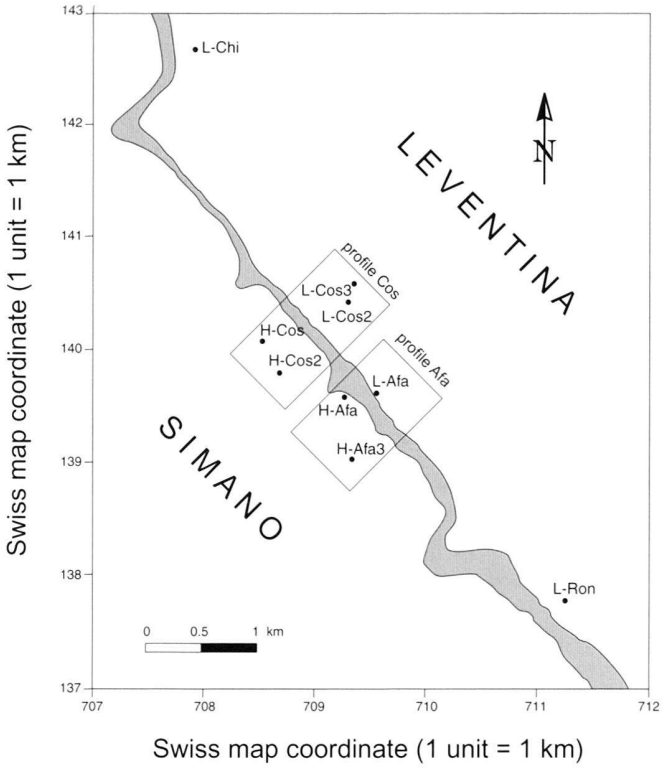

Fig. 7. Tectonic map of the study area showing fission track sample localities and the extent of the mylonite zone between Leventina (below) and Simano nappe (above).

4. Apatite fission track dating

4.1 Sample treatment and methodology

For apatite fission track analyses, ortho- and paragneisses were sampled along two transects across the mylonitic nappe boundary (Fig. 7, transects Cos and Afa), together with two additional samples collected along the Ticino valley bottom. Apatites were separated following standard mineral separation procedures. They were mounted, polished and etched (20 s in 5N HNO_3). Track length measurements on large grain mounts early revealed that most samples contain low concentration of U, in the range of 5–15 ppm. Only one sample (H-Afa, with an average of 25 ppm U) yielded a standard number of 100 track lengths, while another three samples (L-Afa, L-Chi, L-Ron) contained sufficient confined track lengths to allow a preliminary interpretation.

The samples were irradiated at the Lukas Heitz facility, Australia. Mounting and etching (45 min in HF) of the micas were performed at the ETH Zürich FT laboratory. For counting and track length measurements, a Zeiss Axioplan microscope with a computer-driven stage and a digitizing tablet was used at a total magnification of 1600. The assumed accuracy of a single track measurement is estimated to be in the range of 0.05 μm. Central ζ ages were calculated for apatites using freeware provided by M. Brandon (http://www.geology.yale.edu/~brandon/Software/FT_PROGRAMS/index.html). FT data of the apatite samples are summarised in Table 3.

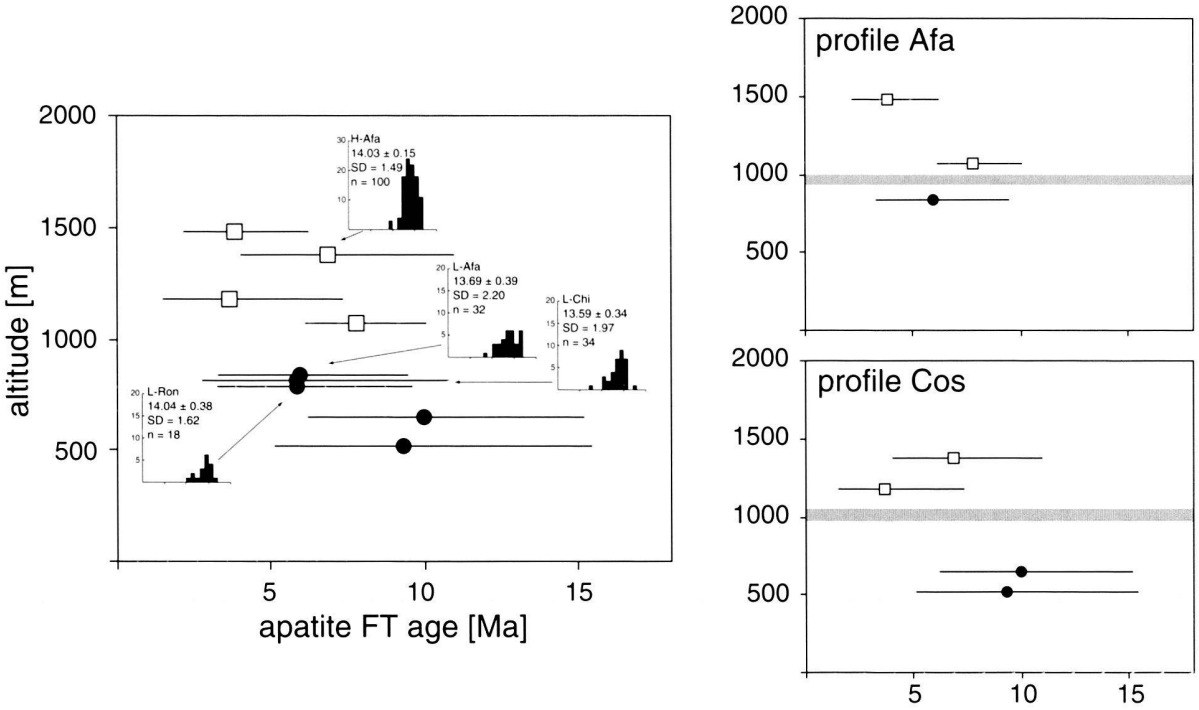

Fig. 8. Age-altitude diagram of the apatite FT ages (with 2σ errors) and FT length histograms from the study area. The small diagrams to the right show the relationship along two separate transects "Afa" and "Cos". For sample localities, see Fig. 7.

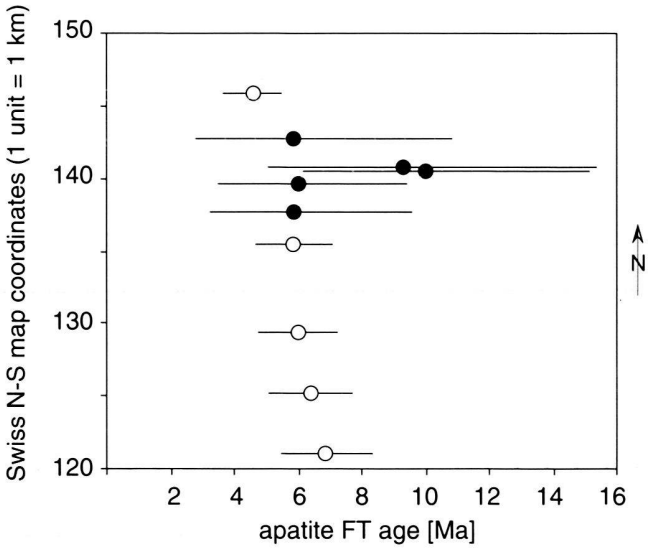

Fig. 9. North-south profile of apatite FT ages following the Ticino valley with data from Wagner et al. (1977) (open circles) and this study (filled circles). The indicated age errors are 2σ, those from Wagner et al. (1977) were assumed to be 20% of the indicated age at a 95% confidence interval.

4.2 FT results

The calculated FT ages vary between 3.7 and 10 Ma. Due to the low U content, most ages have 1σ errors in the range of 20–50%. A correlation of the FT ages from the combined transects with sample altitude suggests a negative age-altitude trend, which is also visible in the separated data sets of both transects (Fig. 8). Due to the large age errors, the age-altitude trend is not statistically significant on a 95% confidence interval, and the age-elevation relationship could also be vertical. At the same confidence level, however, a positive age-elevation relationship is excluded. Along the Ticino valley, apatite FT ages from this study fit into the regional context (Fig. 9) and show a tendency of the ages to become younger upstream.

Mean track lengths vary between 13.6 and 14.1 μm (Tab. 2, Fig. 8). The mean length values and the slightly tailed length distribution (Fig. 8) indicate moderate to fast cooling through the apatite partial annealing zone (PAZ). The sample from the Simano nappe, i.e. from high elevation, has a long mean length and the narrowest length distribution, while those in the valley show stronger tailing in their length distributions. Similar observations were made in the Glarus Alps, and were explained by the separate cooling paths of high elevation and low elevation samples during late-stage exhumation (Rahn & Grasemann 1999). Samples at the valley bottom underwent fast cooling only at temperatures below the apatite PAZ due to condensed isotherms below the valley floors. Samples closer to the summits, however, commonly reveal reduced cooling rates during their final ascent to the surface through the expanded isotherms below topographic heights. Accordingly, the summit

Tab. 2. Apatite fission track analyses from the study area.

Sample No and Tectonic Unit	No. Crystals	Spontaneous ρ_S (N_S)	Induced ρ_i (N_i)	$P\chi^2$	Dosimeter ρ_d* (N_d)	Central FT Age (+1σ/-1σ)	Mean Track Length	S.d. of distribution (No. Tracks)
LEV H-Afa		0.015	0.393	80%	11.58	7.8 Ma	14.03	1.49
Simano nappe	20	(65)	(1667)		(8668)	(-0.9/+1.1)		(100)
LEV H-Afa3		0.004	0.179	93%	11.34	3.9 Ma		
Simano nappe	15	(17)	(854)		(3858)	(-1.0/+1.2)		
LEV H-Cos		0.002	0.102	74%	11.21	3.7 Ma		
Simano nappe	15	(8)	(419)		(8668)	(-1.4/+1.8)		
LEV H-Cos2		0.006	0.174	82%	11.09	6.9 Ma		
Simano nappe	20	(18)	(501)		(8668)	(-1.7/+2.0)		
LEV L-Afa		0.003	0.094	92%	10.85	6.0 Ma	13.69	2.20
Leventina gneiss	20	(19)	(592)		(8739)	(-1.4/+1.7)		(32)
LEV L-Chi		0.002	0.054	53%	10.73	5.9 Ma	13.59	1.97
Leventina gneiss	20	(10)	(319)		(8739)	(-1.9/+2.4)		(34)
LEV L-Cos2		0.004	0.081	80%	10.61	10.0 Ma		
Leventina gneiss	20	(23)	(421)		(8668)	(-2.2/+2.5)		
LEV L-Cos3		0.003	0.061	61%	10.48	9.3 Ma		
Leventina gneiss	20	(15)	(293)		(8668)	(-2.5/+3.0)		
LEV L-Ron		0.003	0.095	53%	10.36	5.9 Ma	14.04	1.62
Leventina gneiss	20	(16)	(491)		(8739)	(-1.5/+1.8)		(18)

Notes:

(i) Track densities are ($x10^7 tr\ cm^{-2}$), *=($x10^5\ tr\ cm^{-2}$) numbers of tracks counted (N) shown in brackets;

(ii) analyses by external detector method using 0.5 for the $4\pi/2\pi$ geometry correction factor;

(iii) ages calculated using dosimeter glass CN-5 for apatite with $\zeta_{CN5} = 344 \pm 5$

(iv) $P(\chi^2)$ is probability for obtaining χ^2 value for v degrees of freedom, where v = no. crystals - 1.

(v) track length data are given in 10^{-6}m, S.d = 1σ standard deviation.

samples had more time to accumulate tracks of full length after complete cooling through the PAZ.

Regardless the unclear age-elevation relationship, there is no discernible offset of ages across the mylonite zone, i.e. the Leventina-Simano nappe boundary. This implies that there was no significant vertical component of displacement across the mylonite zone since the rocks cooled below the apatite PAZ.

5. Discussion

5.1 Regional Quartz texture

The quartz textures and microstructures from the Leventina-Simano nappe boundary suggest deformation at greenschist to lower amphibolite facies metamorphic conditions. By comparing the metamorphic conditions of deformation and micro- and macrostructures, it can be concluded that the deformation along the nappe boundary occurred during the third deformation phase or before (for correlation of successions of the deformation events see Table in Grujic & Mancktelow 1996). This deformation phase is linked to the formation of the north-south trending Maggia Steep zone (Preiswerk 1918; Merle et al. 1989; Grujic & Mancktelow 1996; Steck 1998) and to the formation of the Ticino subdome (Merle et al. 1989). Because of the presence of a mylonite zone overprinted by brittle fractures the nappe boundary, however, apparently resembles major detachment shear zones in the Alps that operated at lower temperature conditions (Mancktelow 1992, Fügenschuh et al. 1997). In the study area evidence of orogen-parallel extension is provided by joints, often associated with chloritisation, by slickenlines along the foliation surfaces and by pseudotachylites (Irouschek & Huber 1982). These structures consistently indicate top-down-to-the WNW sense of shear, similar to the kinematics in the Simplon shear zone (e.g. Steck 1980, 1984, 1987, 1990; Mancktelow 1985, 1990, 1992; Mancel & Merle 1987) and the Brenner shear zone (e.g. Behrmann 1988; Selverstone 1988, 1993; Axen et al. 1995; Selverstone et al. 1995; Fügenschuh et al. 1997) where the ductile shearing occurred during Miocene times. The top-to-the WNW, brittle to plastic structures at the Leventina-Simano boundary have occurred at retrograde temperature conditions (Merle et al.

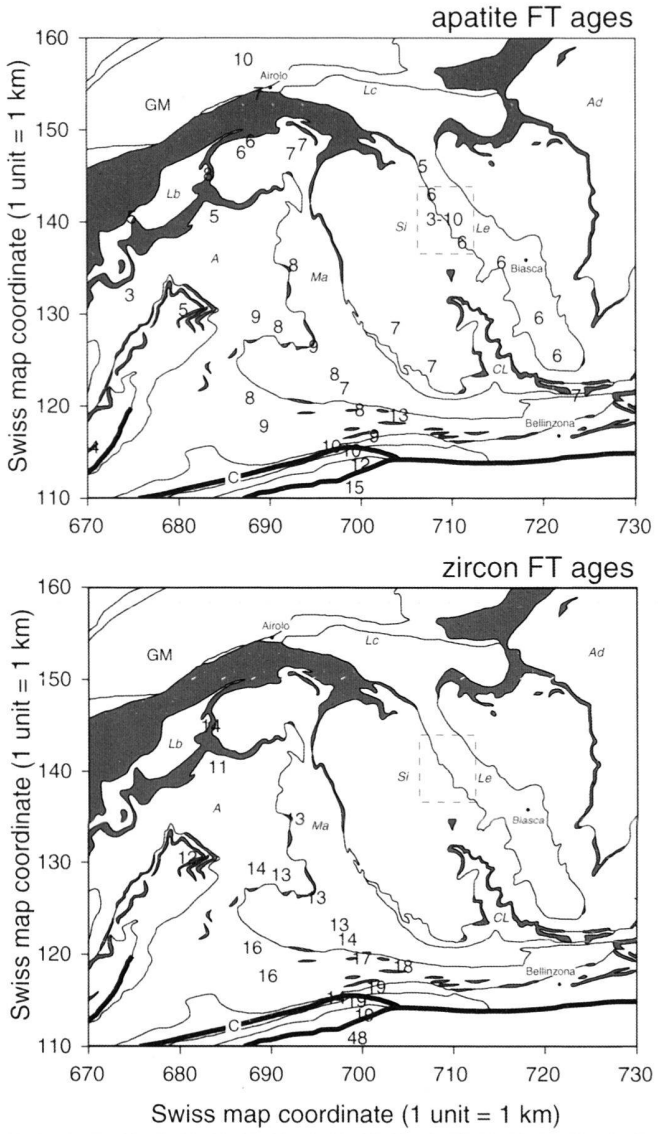

Fig. 10. Overview of published apatite and zircon FT data in the Lepontine area (Wagner & Reimer 1972, Wagner et al. 1977, Steiner 1984, Hurford 1986, this study, ages were rounded to the closest integer). The dashed outline indicates the location of the study area and apatite FT data from within this area are given in Tab. 2. Tectonic sketch map after Spicher (1980).

1989) and clearly postdate the mylonitic foliation. A similar situation has been observed at the Simplon shear zone where the vertical component of displacement was of such magnitude that the earlier deep-seated mylonites were overprinted by higher-level, brittle deformation during the same kinematic event. In the Leventina-Simano boundary, however, the mylonites and the brittle structures have inconsistent kinematics. Nevertheless, it is obvious that some reactivation of the nappe boundary has occurred during the same tectonic phase when the Simplon and Brenner shear zones were active.

In the Lepontine Alps the macroscopic stretching lineation L_2 (finite strain feature) and the kinematic directions inferred from the quartz textures have different orientations (Grujic 1991). Similar to the situation in the Leventina and Simano nappes, the *c*-axis pattern in the Wandfluhhorn fold (to the west of the Leventina valley) is oblique to the macroscopic lineation (Klaper 1988). The Wandfluhhorn fold is a tight recumbent fold that affects the main foliation (S_2) in the Lepontine Alps (Hall 1972) and has been interpreted by Milnes (1974) as the most important post-nappe structure in the Lepontine Alps. The associated axial planar crenulation cleavage is subhorizontal, and dips to the ESE. The fold hinge trends 100/20 (Hall 1972) and is coaxial to an older stretching lineation, which is inferred to be a D_2 feature, (Grujic & Mancktelow 1996). Steck (1998) considers the Wandfluhhorn fold as an antiformal syncline that is of the same phase as the Maggia crossfold. In both limbs of the Wandfluhhorn fold the kinematic direction *X* determined from *c*-axis patterns is at 30° to 50° to the macroscopic stretching lineation and thus trends towards northeast to east (60° – 80°) (Klaper 1988). There is also a systematic change in inferred shear sense. In the lower limb of the Wandfluhhorn fold (western area) the shear sense is top-to-the-SW; in the upper limb (eastern area) the shear sense is top-to-the-NE. In addition, textures closer to the axial plane indicate a dominant pure shear component of deformation, while the simple shear component increases away from the axial plane. Klaper (1988) has tentatively proposed that the quartz texture might be a pre- or early syn-Wandfluhhorn fold feature. The quartz texture and microstructures at the Leventina-Simano nappe boundary are similar to those in the Wandfluhhorn fold and suggest similar deformation conditions. In lack of other information it is, however, not possible to deduce whether the textures in the two areas are contemporaneous or not. Nevertheless, combining the observations from the two areas, we argue that the quartz texture in the Leventina valley is a late- or post-D_2 feature. The quartz texture from the nappe boundary could be associated with the D_3 regional event that lead to the formation of the Maggia Steep zone (Preiswerk 1921; Merle et al. 1989; Grujic & Mancktelow 1996; Steck 1998) and the Ticino subdome (Merle et al. 1989).

In the study area a top-to-the-WNW shear took place under brittle conditions. This is confirmed by the widespread slickenlines on the foliation planes, joints and pseudotachylites, mainly within the mylonite zone (Fig. 3). This fact demonstrates the difference between the mylonite zone in the study area and the Simplon shear zone. The Simplon zone consists of a several kilometre broad zone of mylonites that shows an amphibolite to greenschist facies stretching lineation dipping to the SW overprinted locally by brittle features with the same kinematics (Steck 1980, 1990; Mancktelow 1990, 1992; Steck & Hunziker 1994).

5.2 Apatite fission track data

The apatite FT data are consistent with moderate to fast exhumation of the area during the upper Miocene and Pliocene.

They suggest a negative vertical trend of FT ages within a horizontal distance of less than 2 km. In the Lepontine dome, published apatite FT ages (Wagner & Reimer 1972, Wagner et al. 1977, Steiner 1984, Hurford 1986, Soom 1990, this work) vary between 3 and 13 Ma (Fig. 10), and most of this spread is found at the investigated nappe boundary. In the Lepontine dome, Pliocene ages are also found along the Simplon fault footwall (3–5 Ma, Soom 1990), and the Ticino valley (4–10 Ma, Hurford 1986), while the oldest ages are found in the vicinity of the Insubric line (8–13 Ma). Zircon FT ages vary between 11 and 19 Ma (Fig. 10). Both apatite and zircon FT ages from the Lepontine dome show an increase from N to S. This low-temperature age pattern suggests that since the Middle Miocene the Lepontine "dome" did not undergo a typically domal exhumation that would lead to young ages in the centre and old ages towards to domal rim. The apatite and zircon FT pattern in Lepontine dome is asymmetric with the youngest ages in the W (Simplon fault) and N (Penninic front), which suggests a strong relationship between late-stage exhumation and movements along major fault systems (Soom 1990, Grasemann & Mancktelow 1993; Steck & Hunziker 1994). Exhumation in the eastern Lepontine is characterized by subdomes such as the Ticino subdome that culminates above the Ticino valley (Fig. 1). This is consistent with our structural interpretation, which indicates that the Lepontine dome is a composite structure in which the steep flanks of the dome were products of various deformational events, and the planar fabrics delineating the dome are of different age (e.g. Grujic & Mancktelow 1996).

The age-elevation trend in the Leventina Valley seems to be inconsistent with the commonly positive age-elevation relationship in the Alps (e.g. Schär et al. 1975, Rahn & Grasemann 1999). The interpretation of the data is limited due to the large age errors. Assuming the negative age-elevation trend to be real for the time being, three potential interpretations may be considered:

a) The observed age-elevation pattern may be the effect of very late movements along the shear zone between the two nappes. This would be consistent with the positive nappe-internal trends of the Cos profile (Fig. 8), but inconsistent with the here presented structural data, which show no evidence of late thrusting.
b) The negative age-elevation relationship may be the result of profile tilting after closure of the apatite FT system. By tilting, a former positive age-elevation slope could have become steeper, and eventually overturned into a negative slope. The process does not require late movements along the Leventina-Simano nappe boundary but a gradient in exhumation between sampled valley bottom and slope. Such a gradual increase in exhumation may be due to normal faulting along the Simplon fault system. However, major activities along the Simplon fault occurred in the early and middle Miocene (Grasemann & Mancktelow 1993, Steck & Hunziker 1994), and the post-10 Ma Simplon fault-related exhumation would be insufficient to explain the amount of tilting required in the Ticino valley.
c) The negative age-elevation trend may be due to the interaction between landscape evolution and exhumation (Stüwe et al. 1994, Mancktelow & Grasemann 1997). A decrease in relief has been proposed to cause a significant steepening or overturning of the age-elevation relationship (Braun 2002). Alternatively, a lateral shift of the valley could have lead to localised high exhumation rates (Stüwe & Hintermüller 2000) and therefore steep local isotherms during apatite FT closure. Depending on the time of local doming of the Leventina-Simano nappe boundary, the coincidence of the hinge of the Ticino subdome and the Ticino valley (Fig. 1) may be used as an additional argument for an interlude between exhumation and fluvial erosion. In such case the formation of the Ticino subdome may have been the cause for local erosion-driven exhumation and the recorded ages would indicate the time of doming.

In summary, none of the discussed potential interpretations for the negative age-elevation trend is fully satisfying. The lack of significant brittle deformation along the shear zone between Simano and Leventina nappe (required by interpretation a) or large-scale exhumation along normal faults (necessary to support interpretation b) excludes any tectonic explanation for the apatite FT age pattern. The influence of apatite composition as a cause for the negative age-elevation relationship is difficult to disprove due to very low track densities, and the resulting lack of statistically significant measurements of etch pit diameters (Carlson et al. 1999). The currently most likely explanation for the negative age-elevation relationship suggests an influence of topography and local differences in exhumation on the shape of the near-surface palaeo-isotherms. However, there is currently a lack of other evidence to support such a model of a strong deformation of the isotherms within the last 10 myr. A much larger and more precise set of low-temperature geochronological data (FT, U/Th-He) would be needed for a more profound interpretation of our data.

6. Conclusions

The analysis of quartz tectonites at the boundary between the Leventina and the Simano nappe throws light on the progressive deformation history and the conditions that prevailed during shear zone formation. The nappe boundary was a site of high strain concentration during deformation at protracted peak temperature conditions. This resulted in the formation of a ductile mylonite zone along the nappe boundary.

The last ductile increment of the progressive deformation recorded by the quartz textures took place at intermediate temperature conditions of ~400 to ~630 °C. The reconstructed shear directions show a considerable trend variation in the study area (Fig. 11). The spread could possibly be explained by a coaxial component of the bulk general shear deformation geometry, perhaps related to the vertical shortening of the nappe pile and concomitant radial stretching. This vertical component may have been related to the crustal overthicken-

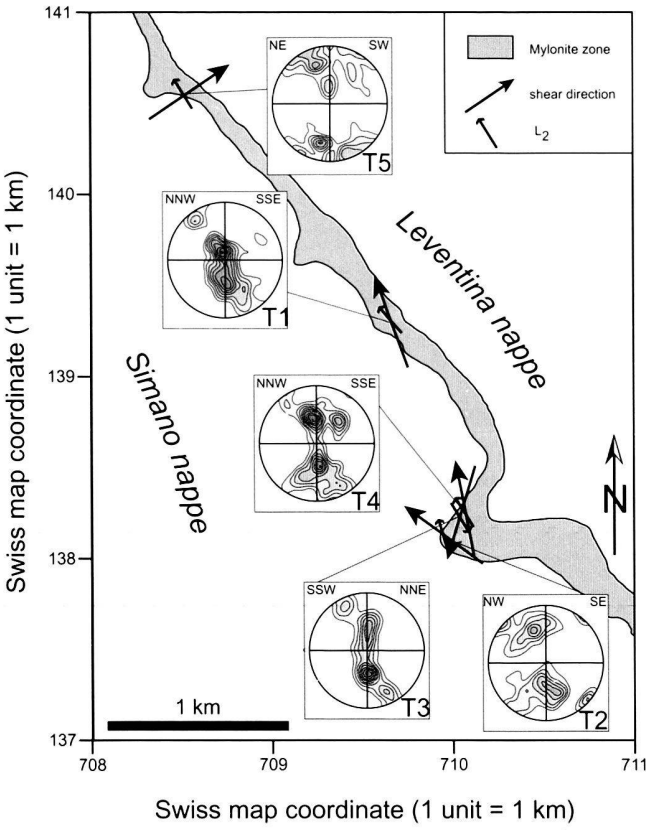

Fig. 11. Shear directions in the hanging wall revealed by quartz texture analysis. Middle of arrow corresponds to sample locality.

ing within the central part of the Alpine orogen by bivergent (retro- and pro-wedge) thrusting (Schmid & Kissling 2000). The topology of *c*-axis diagrams, however, does not support the idea of general shear. Only two samples may be indicative of flattening strain conditions. On the basis of the kinematic and metamorphic conditions, the ductile deformation that caused the crystallographic preferred orientation in the quartz tectonites is assigned to the late-second to third regional deformation phase (D_2, D_3 in Huber et al. 1980; and in Grujic & Mancktelow 1996; HTD in Merle et al. 1989). Reactivation of the mylonite zone, with top-to-the-WNW shear took place under brittle to brittle-ductile conditions. Thereby brittle-ductile shear bands, discrete shear fractures and pseudotachylites were formed. This shearing is possibly in kinematic connection with the orogen-parallel extensional event during Miocene.

Apatite FT data across the nappe boundary reveal ages similar to the regional age pattern (Wagner et al. 1977, Hurford 1986). The steeply negative age-elevation trend cannot be explained by late-stage movements along the shear zone between Simano and Leventina nappe, but is more likely an effect of changing topography and its impact on the palaeo-isotherms at depths within the apatite FT partial annealing zone.

The FT data combined with structural and kinematic data indicate that there was no considerable amount of vertical displacement along the Leventina-Simano nappe boundary during or after Mid Miocene. This study raises the question whether the observed curvature of the Leventina-Simano nappe boundary may alternatively be explained by local late-stage erosion-driven exhumation, on top of a former Ticino subdome (sensu Merle et al. 1989).

Neither the horizontal displacement along the shear zone, nor the vertical shortening could be constrained by the FT data. Nevertheless, the structural and FT data show that this nappe boundary is a long-lived high strain zone that has been multiply reactivated through its Alpine history. A similar deformation history is expected for the other Alpine nappe boundaries. Their cumulative strain, at different deformation phases, could be considerable and thus should be taken in account in tectonic reconstructions of the central Alps. Finally, the feedback between tectonic and surface processes is becoming increasingly appreciated and understood (e.g. Willett et al. 1993; Beaumont et al. 2001; Kohn & Green 2002; Willett & Brandon 2002) and, although disputed (Molnar 2003) implies that the topography carries information on the recent tectonic activities, and the low-temperature geochronology may convey information for both aspects of evolution of an active orogen.

Acknowledgements

Quartz texture analysis presented in this paper was part of the Diploma thesis of Z. Timar-Geng at the University of Freiburg, Germany. He is particularly grateful to Prof. J. Behrmann for introducing him to the technique of U-stage measurement. Mineral separation was done by N. Kindler, IMPG Freiburg. FT investigations were supported by grant Ra 704/3-1 of the Deutsche Forschungsgemeinschaft. We gratefully acknowledge the critical reading of the manuscript and the constructive comments by S. Schmid, H. Stünitz and A. Steck. We would like to thank D. Seward for her open door at the ETH Zürich FT laboratory.

REFERENCES

Axen, G.J., Bartley, J.M. & Selverstone, J. 1995: Structural expression of a rolling hinge in the footwall of the Brenner Line normal fault, eastern Alps. Tectonics 14, 1380–1392.

Beaumont, C., Jamieson, R. A., Nguyen, M.H. & Lee, B. 2001: Himalayan tectonics explained by extrusion of a low-viscosity crustal channel coupled to focused surface denudation, Nature 414, 738–742.

Behrmann, J. 1988: Crustal-scale extension in a convergent orogen: The Sterzing-Steinach mylonite zone in the eastern Alps. Geodin. Acta 2, 63–73.

Behrmann, J.H. & Platt, J.P. 1982: Sense of nappe emplacement from quartz c-axis fabrics: an example from the Betic Cordilleras (Spain). Earth Planet. Sci. Lett. 59, 208–215.

Bernet, M., Zattin, M., Garver, J.I., Brandon, M.T. & Vance, J.A. 2001: Steady-state exhumation of the European Alps. Geology 29/1, 35–38.

Bouchez, J.-L. & Pêcher, A. 1981: The Himalayan Main Central Thrust pile and its quartz-rich tectonites in central Nepal. Tectonophysics 78, 23–50.

Braun, J. 2002: Quantifying the effect of recent relief changes on age-elevation relationships. Earth Planet. Sci. Lett. 200, 331–343.

CARLSON, W.D., DONELICK, R.A. & KETCHAM, R.A. 1999: Variability of apatite fission-track annealing kinetics: I. Experimental results. Amer. Mineralogist 84 (9), 1213–1223.

CASASOPRA, S. 1939: Studio petrografico dello Gneiss granitico Leventina (Valle Riviera e Valle Leventina, Canton Ticino). Schweiz. Mineral. Petrogr. Mitt. 19, 449–709.

FREY, M. & FERREIRO MÄHLMANN, R. 1999: Alpine metamorphism of the Central Alps. Schweiz. Mineral. Petrogr. Mitt. 79, 1–4,135–154.

FÜGENSCHUH, B., SEWARD, D. & MANCKTELOW, N. 1997: Exhumation in a convergent orogen: the western Tauern window. Terra Nova 9, 213–217.

FROITZHEIM, N., SCHMID, S.M. & FREY, M. 1996: Mesozoic paleogeography and the timing of eclogite-facies metamorphism in the Alps: A working hypothesis. Eclogae Geol. Helv. 89, 81–110.

GRASEMANN, B. & MANCKTELOW, N.S. 1993: Two-dimensional thermal modelling of normal faulting: the Simplon Fault Zone, Central Alps, Switzerland. Tectonophysics 225, 155–165.

GRASEMANN, B., FRITZ, H. & VANNAY, J.-C. 1999: Quantitative kinematic flow analysis from the Main Central Thrust Zone (NW-Himalaya, India): implications for a decelerating strain path and the extrusion of orogenic wedges. J. Struct. Geol. 21, 837–853.

GRUJIC, D. 1991. Fold interference patterns and quartz *c*-axis fabrics in the Maggia nappe, Lower Penninic nappes, Switzerland. 6th meeting of the European Union of Geosciences, Strasbourg, Terra abstracts, 3, 360.

GRUJIC, D. & MANCKTELOW, N.S. 1996: Structure of the northern Maggia and Lebendun Nappes, Central Alps, Switzerland. Eclogae Geol. Helv. 89/1, 461–504.

HALL, W.D.M. 1972: The structural geology and metamorphic history of the lower Pennine nappes, Valle di Bosco, Ticino, Switzerland. Unpubl. Ph.D. thesis, Univ. of London.

HEILBRONNER, R. & TULLIS, J. 2002: The effect of static annealing on microstructures and crystallographic preferred orientations of quartzites experimentally deformed in axial compression and shear. In: DE MEER, S., DRURY, M.R., DE BRESSER, J.H.P. & PENNOCK, G.M. (Eds.). Deformation mechanisms, rheology and tectonics; current status and future perspectives. Spec. Publ. Geol. Soc. London 200, 191–218.

HUBER, M., RAMSAY, J.G. & SIMPSON, C. 1980: Deformation in the Maggia and Antigorio nappes, Lepontine Alps. Eclogae Geol. Helv. 73, 593–606.

HURFORD, A.J. 1986: Cooling and uplift patterns in the Lepontine Alps, South Central Switzerland, and an age of vertical movement on the Insubric fault line. Contr. Mineral. Petrol. 92, 413–427.

HURFORD, A.J., FLISCH, M. & JÄGER, E. 1989: Unravelling the thermo-tectonic evolution of the Alps; a contribution from fission track analysis and mica dating. Spec. Publ. Geol. Soc. London 45, 369–398.

IROUSCHEK, A. & HUBER, M. 1982: Pseudotachylite zones in the Leventina Gneiss (Lepontine Alps, Ticino, Switzerland). Schweiz. Mineral. Petrogr. Mitt. 62, 313–325.

JÄGER, E. 1973: Die Alpine Orogenese im Lichte der Radiometrischen Altersbestimmung. Eclogae Geol. Helv. 66, 11–21.

KLAPER, E.M. 1988: Quartz *c*-axis fabric development and large-scale post-nappe folding (Wandfluhhorn Fold, Penninic nappes). J. Struct. Geol. 10/8, 795–802.

KOHN, B. P. & GREEN, P. F. 2002: Low temperature thermochronology; from tectonics to landscape evolution. Tectonophysics 349, 1–365.

KRETZ, R. (1983): Symbols for rock-forming minerals. Amer. Mineralogist 68, 277–279.

KUHLEMANN, J., FRISCH, W., DUNKL, I. & SZÉKELY, B. 2001: Quantifying tectonic versus erosive denudation by the sediment budget: the Miocene core complexes of the Alps. Tectonophysics 330, 1–23.

LAW, R.D. Crystallographic fabrics: a selective review of their applications to research in structural geology 1990. In: KNIPE, R.J. & RUTTER, E.H. (Eds). Deformation Mechanisms, Rheology and Tectonics. Spec. Publ. Geol. Soc. London 54, 335–352.

MANCEL, P. & MERLE, O. 1987: Kinematics of the northern part of the Simplon Line (Central Alps). Tectonophysics 135, 265–275.

MANCKTELOW, N.S. 1985: The Simplon line; a major displacement zone in the western Lepontine Alps. Eclogae Geol. Helv. 78, 73–96.

– 1987: Quartz textures from the Simplon Fault Zone, southwest Switzerland and north Italy. Tectonophysics 135, 133–153.

– 1990: The Simplon Fault Zone. Beitr. Geol. Karte Schweiz N.F. 163.

– 1992: Neogene lateral extension during convergence in the Central Alps: evidence from interrelated faulting and backfolding around the Simplon-pass (Switzerland). Tectonophysics 215, 295–317.

MANCKTELOW, N.S. & GRASEMANN, B. 1997: Time-dependent effects of heat advection and topography on cooling histories during erosion. Tectonophysics 270, 167–195.

MERLE, O., COBBOLD, P.R. & SCHMID, S. 1989: COWARD, M.P., DIETRICH, D. & PARK, R.G. (Eds.). Tertiary kinematics in the Lepontine dome. In: Alpine Tectonics. Spec. Publ. Geol. Soc. London 45, 113–134.

MEYRE, C., MARQUER, D., SCHMID, S.M. & CIANCALEONI, L. 1998: Syn-orogenic extension along the Forcola fault: Correlation of Alpine deformations in the Tambo and Adula nappes (Eastern Penninic Alps). Eclogae Geol. Helv. 91, 409–420.

MILNES, A.G. 1974: Post-nappe folding in the western Lepontine Alps. Eclogae Geol. Helv. 67, 333–348.

MOLNAR, P. 2003: Nature, nurture and landscape. Nature, 426, 612–614.

NIEVERGELT, P., LINIGER, M., FROITZHEIM, N. & FERREIRO MÄHLMANN, R 1996: Early to mid Tertiary crustal extension in the Central Alps; the Turba mylonite zone (eastern Switzerland). Tectonics 15/2, 329–340.

NIGGLI, P., PREISWERK, H., GRÜTTER, O., BOSSARD, L. & KÜNDIG, E. 1936: Geologische Beschreibung der Tessiner Alpen zwischen Maggia- und Bleniotal. Beitr. Geol. Karte Schweiz N.F. 71.

PASSCHIER, C.W. & TROUW, R. 1998: Microtectonics. Springer-Verlag 1996/1998. 2nd corrected reprint 1998.

PREISWERK, H. 1918: Geologische Beschreibung der Lepontinischen Alpen –zweiter Teil: Oberes Tessin und Maggiagebiet. Beitr. geol. Karte Schweiz 26, 80.

– 1921: Die zwei Deckenkulminationen Tosa-Tessin und die Tessiner Querfalte. Eclogae Geol. Helv. 16, 485–496.

RAHN, M.K. & GRASEMANN, B. 1999: Numerical and Monte-Trax modeling on fission track data from the Glarus Alps: Thermal and tectonic evolution of a thrust plane during metamorphism and exhumation. Earth Planet. Sci. Lett. 169, 245–259.

RÜTTI, R. 2001: Tectono-metamorphic evolution of the Simano-Adula nappe boundary, Central Alps, Switzerland. Schweiz. Mineral. Petrogr. Mitt. 81, 115–129.

RÜTTI, R., MANCKTELOW, N.S., THOMPSON, A.B. & MARQUER, D. 2001: Tectono-Metamorphic Evolution of the Simano Nappe at Alpe Sponda, Central Alps, Switzerland. J. Conf. Abstracts (EUG XI) 6/1, 629.

SCHÄR, J.-P., REIMER, G.M. & WAGNER, G.A. 1975: Actual and ancient uplift rate in the Gotthard region, Swiss Alps; a comparison between precise levelling and fission-track apatite age. Tectonophysics 29, 293–300.

SCHLUNEGGER, F. & WILLETT, S. 1999: Spatial and temporal variations in exhumation of the Swiss Alps and implications for exhumation mechanisms. Spec. Publ. geol. Soc. London 154, 157–179.

SCHMID, S.M. 1994: Textures of geological materials: computer model predictions versus empirical interpretations based on rock deformation experiments and field studies. In: BUNGE, H.J., SIEGESMUND, S., SKROTZKI, W. & WEBER, K. (Eds.). Textures of Geological Materials. DGM Informationsgesellschaft, Oberursel, 279–302.

SCHMID, S.M. & CASEY, M. 1986: Complete fabric analysis of some commonly observed quartz c-axis patterns. In: HOBBS, B.E. & HEARD, H.C. (Eds.). Mineral and Rock Deformation: Laboratory Studies – The Paterson Volume. AGU, Geophys. Monogr. 36, 263–286.

SCHMID, S.M. & KISSLING; E. 2000: The arc of western Alps in the light of geophysical data on deep crustal structure. Tectonics 19, 62–85.

SELVERSTONE, J. 1988: Evidence for east-west crustal extension in the eastern Alps: Implications for the unroofing history of the Tauern Window. Tectonics 7, 87–105.

– 1993: Micro- to macroscale interactions between deformational and metamorphic processes, Tauern Window, Eastern Alps. Schweiz. mineral. petrog. Mitt. 73, 229–239.

SELVERSTONE, J., AXEN, G.J. & BARTLEY, J.M. 1995: Fluid inclusion constraints on the kinematics of footwall uplift beneath the Brenner Line normal fault, eastern Alps. Tectonics 14, 264–78.

SIMPSON, C. & SCHMID, S.M. 1982: Some useful criteria for shear sense determination in mylonites. Abstracts with Programs – Geol. Soc. Am. 14/7, 618.

SOOM, M.A. 1990: Abkühlungs- und Hebungsgeschichte der Externmassive und der penninischen Decken beiderseits der Simplon-Rhone-Linie seit dem Oligozän: Spaltspurdatierungen an Apatit/Zirkon und K-Ar-Datierungen an Biotit/Muskovit (Westliche Zentralalpen). Ph. D. thesis, University of Bern, 119p.

SPICHER, A. 1980: Tektonische Karte der Schweiz 1: 500 000. 2. Ausgabe. Schweiz. Geol. Komm., Wabern.

STECK, A. 1980: Deux directions principales de flux synmétamorphiques dans les Alpes centrales. Bull. Soc. Vaudoise Sci. Nat. 75, 141–149.

– 1984: Structures de déformation tertiaires dans les Alpes centrales (transversale Aar-Simplon-Ossola). Eclogae Geol. Helv. 77, 55–100.

– 1987: Le massif du Simplon – Réflexions sur la cinématique des nappes de gneiss. Schweiz. Mineral. Petrogr. Mitt. 67, 27–45.

– 1990: Une carte des zones de cisaillement ductile des Alpes Centrales. Eclogae Geol. Helv. 83, 603–627.

– 1998: The Maggia cross-fold: An enigmatic structure of the Lower Penninic nappes of the Lepontine Alps. Eclogae Geol. Helv. 91/3, 333–343.

STECK, A. & HUNZIKER, J. 1994: The Tertiary structural and thermal evolution of the Central Alps – compressional and extensional structures in an orogenic belt. Tectonophysics 238, 229–254.

STEINER, H. 1984: Radiometrische Altersbestimmungen an Gesteinen der Maggia-Decke (Penninikum der Zentralalpen). Schweiz. Mineral. Petrogr. Mitt. 64, 227–259.

STIPP, M., STÜNITZ, H., HEILBRONNER, R. & SCHMID, S.M. 2002: Dynamic recrystallization of quartz: correlation between natural and experimental conditions. In: DE MEER, S., DRURY, M.R., DE BRESSER, J.H.P. & PENNOCK, G.M. (Eds.). Deformation Mechanisms, Rheology and Tectonics: Current status and Future Perspectives. Geol. Soc. London, Spec. Publ. 200, 171–190.

STÜWE, K., WHITE, L. & BROWN, R. 1994: The influence of eroding topography on steady-state isotherms. Application to fission-track analysis. Earth Planet. Sci. Lett. 124, 63–74.

STÜWE, K. & HINTERMÜLLER, M. 2000: Topography and isotherms revisited: the influence of laterally migrating drainage divides. Earth Planet. Sci. Lett. 184, 287–303.

TODD, C.S. & ENGI, M. 1997: Metamorphic field gradients in the Central Alps. J. Metamorphic Geol. 15, 513–530.

TRÜMPY, R. 1980: Geology of Switzerland – a guide-book. Part A: An Outline of the Geology of Switzerland. Ed. by Schweizerische Geologische Kommission. Wepf & Co. Publishers, Basel, New York.

VON EYNATTEN, H., SCHLUNEGGER, F., GAUPP, R. & WIJBRANS, J.R. 1999: Exhumation of the Central Alps: evidence from $^{40}Ar/^{39}Ar$ laserprobe dating of detrital white micas from the Swiss Molasse Basin. Terra Nova 11/6, 284–289.

WAGNER, G.A. & REIMER, G.M. 1972: Fission track tectonics: the tectonic interpretation of fission track ages. Earth Planet. Sci. Lett. 14, 263–268.

WAGNER, G.A., REIMER, G.M. & JÄGER, E. 1977: Cooling ages derived by apatite fission-track, mica Rb-Sr and K-Ar dating: The uplift and cooling history of the Central Alps. Mem. Ist. Geol. Mineral. Univ. Padova 30, 27p.

WILLETT, S.D., BEAUMONT, C. & FULLSACK, P. 1993: Mechanical model for the tectonics of doubly vergent compressional orogens. Geology 21, 371–374.

WILLETT, S. D. & BRANDON, M. T. 2002: On steady states in mountain belts. Geology 30, 175–178.

Manuscript received December 13, 2002
Revision accepted May 3, 2004